Direct Cortical Representation of Drawing

Andrew B. Schwartz

How the intention to act results in movement is a fundamental question of brain organization. Recent work has shown that this operation involves the cooperative interaction of large neuronal populations. A population vector method, by transforming neuronal activity to the spatial domain, was used to visualize the motor cortical representation of the hand's trajectory made by rhesus monkeys as they drew spirals. Hand path was accurately reflected by a series of population vectors calculated throughout the task. A psychophysical rule relating speed to curvature, the "power law," was found in this cortical representation. The relative timing between each population vector and the corresponding portion of the movement was variable. The population vectors only preceded the movement in a predictive manner in portions of the spiral where the radius of curvature was greater than 6 centimeters. These results show that the movement trajectory is an important determinant of motor cortical activity and that this aspect of motor cortical activity may contribute only to discrete portions of the drawing movement.

Detecting a coherent signal that might represent the control of behavioral output from a system as complex as the central nervous system (CNS) is a difficult task. Cells in many different brain structures change their firing rates in relation to some aspect of movement. Motor cortex cells change their rate of discharge in a way that is dependent on the direction of movement (*1*). Although each cell fires maximally for movements made in a single "preferred direction," the relation between discharge and direction is coarse because a given cell's dynamic range encompasses all movement directions. The population vector algorithm, by combining the activity of many cells, yields a vector sum of preferred directions weighted by each cell's discharge rate (*2*). This vector points in the direction of the physical movement, has a length that corresponds to the movement speed, and may also represent aspects of the intention to move (*3*, *4*).

The experiments in this report were designed to investigate how movement generation operates within a behavioral task. Drawing tasks were used because the trajectory of the hand is constrained behaviorally throughout the task. Motor cortical cell activity was recorded and a series of population vectors calculated at equal time intervals as the figure was drawn. This set of vectors is hypothesized to be a central representation of the figure to be drawn and should have the same spatial and temporal characteristics as the trajectory of the hand. Psychophysical studies have shown that the rate at which a figure is drawn depends on its shape, so that the hand slows in portions of the figure with higher curvature. Generally, as the arm moves through space, its speed is inversely related to the curvature of its path. This relationship has been termed the "⅔ power law" and its more precise relation is

$$A(t) = kC(t)^{2/3}$$

where $A(t)$ is angular velocity and curvature is $C(t)$ (*5*, *6*). This law and others defined through psychophysics describe rules that are thought to be "invariant," with the implication that these features are important to the motor system. The presence of these laws in the activity of different CNS structures can be indicative of the route used to assemble the motor control signal.

Division of Neurobiology, Barrow Neurological Institute, 350 West Thomas Road, Phoenix, AZ 85013, USA.

To examine how the shape of drawing is represented in the motor cortex, two monkeys were trained to make smooth, graceful movements on a touch-sensitive screen. Single cells were recorded (n = 349) from the proximal arm area of the motor cortex. After each cell potential was isolated, the animal performed the "center->out" task from a center position to one of eight targets spaced equally around a circle (6-cm radius) so that the cell's preferred direction could be calculated (*7*). Spirals (7.5-cm outside radius, 1.5-cm inside radius, three cycles) were then drawn (*8*).

Neuronal population vectors calculated from single-unit activity (*9*) recorded during the spiral task are hypothesized to represent the hand's trajectory. Spike data recorded for each cell were divided into 100 bins over the duration of the task. For each bin starting from movement onset, a population vector summed across all cells was generated. Finger trajectory data recorded as each neuron was studied were normalized into 100 values corresponding to the spike bins and averaged across cells. Population and tangential velocity vectors are compared in Fig. 1A. The time series start on the left and the origins are aligned vertically. Although local shifting along the time axis would increase their correspondence, the lengths and directions of the population and movement vectors are nearly identical. This finding supports previous sinusoid drawing results (*4*) and

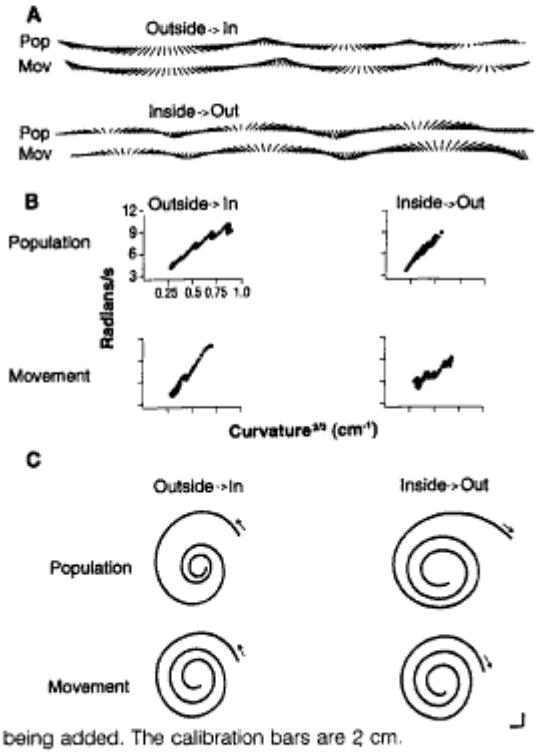

Fig. 1. The time series of population vectors closely reflects the path of the finger. Tangential velocity vectors (Mov) for each bin are compared to the corresponding population vectors (Pop) in (**A**). The origins of the 100 vectors are evenly spaced along the abscissa. The comparison on the top is for the spiral that was drawn from outside->in, whereas that shown in the bottom was for the spiral drawn from inside->out. The vector directions would correspond best if there was a shift along the abscissa for local regions of the display. (**B**) Scatter plot of angular velocity versus curvature$^{2/3}$. Angular velocity, the rate of change in direction of each vector (radians/s), and curvature (cm), the change in direction divided by arc length, were calculated for each bin. The scale is the same for each plot. The first 10 and the last 10 points were omitted in this analysis to avoid acceleration-related effects when starting and stopping the task. (**C**) The population and movement trajectories were created by connecting the vectors tip-to-tail. The directions and magnitudes of the vectors were smoothed before being added. The calibration bars are 2 cm.

shows that a time series of population vectors can represent the tangential velocity or trajectory of the movement.

To test the power law, curvature to the ⅓ power was plotted as a function of angular velocity (Fig. 1B) (*10*). The relation was linear ($r > 0.91$) for both the population and the movement vectors. This shows that the kinematic-figural relation dictated by the power law in humans is also present in monkeys and that it is represented in motor cortical activity.

To better visualize this trajectory representation, the paths represented by these vectors were constructed. The movement and the population vectors were connected tip-to-tail, resulting in the paths shown in Fig. 1C. Comparison to the actual path again confirms the usefulness of the population vector algorithm in generating an isomorphic representation of the trajectory.

These data can also be used to better understand how the information represented at the motor cortex may be incorporated into the movement. Magnitudes and directions of both the movement and population vectors changed continuously during the drawing of each spiral. The directions of the population vectors are very similar to those of the velocity vectors (Fig. 2A). However, there is a small but consistent difference between the movement and population vectors. At the beginning of the outside->in spiral, the directions of the population and movement vectors are almost identical. As more of the spiral was drawn, the time difference (distance between traces along the abscissa) became greater. The reverse effect is observed for the spiral drawn from inside->out.

This time difference, Δt, between corresponding vectors was calculated by finding the time value of the movement direction that corresponded to each population vector direction. A distinctive pattern becomes evident when curvature is plotted as a function of Δt directly (Fig. 2B). For both spirals, Δt begins to increase steeply at about the same value of curvature (0.16) that is equivalent to a 6-cm radius. Below this value, the time difference is small or even negative. The finding that the population vector direction occurs simultaneously with or after movement in that direction suggests that motor cortical activity does not contribute to direction specification in the straighter portions of the movement. The population vectors only predict movement direction for curves with radii of less than 6 cm. When the curvature is in this range, the population vector direction precedes that of the movement by 100 to 120 ms. When the curvature of the drawing exceeds a threshold value, the motor cortical representation leads the movement by a large interval and may be causal in this portion of the movement.

This temporal shift affects the spatial representation of the motor cortical prediction. Each vector's magnitude can be thought of as speed (*4*) and therefore as a combination of space and time (Fig. 3). The helix on the left is a comparison of the neuronal representation (red) to the actual (blue) outside->in spiral. At the bottom of the figure, the spiral is of low curvature and the two paths are very similar. At the top, however, this time difference leads to a distinct difference between the actual and neural trajectories. When Δt is added to each bin along the time axis, the match is better in the region of higher curvature, as represented in the helix on the right.

The neuronal population vectors calculated during this task obeyed the power law derived from psychophysical experiments. Processing responsible for this relation occurs before this information leaves the motor cortex and suggests that the motor cortex or structures that provide afferents to it (or both) generate this kinematic relation. In contrast, the directions encoded by the motor cortex only contribute to the drawing movement when the path to be generated surpasses a minimum curvature. This likely means that the movement information generated by other brain structures follows a route that bypasses the motor cortex for straighter portions of the movement.

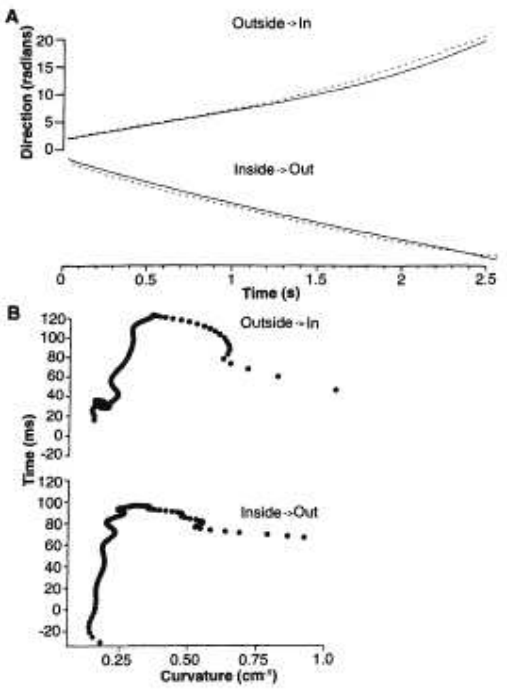

Fig. 2. Comparison of direction between population and movement vectors. (**A**) The population vector directions are represented with the dashed line and the solid line represents the movement vector directions. The bin width was determined by taking the average duration of the task and dividing by the number of bins (99). The average duration of the outside->in spiral was 2485 ms and for the inside->out task it was 2564 ms. The time between corresponding directions of the population and movement vectors was calculated for each time bin. This is the difference along the abscissa between the dashed and solid lines. This time difference, Δt, tended to increase for the outside->in spiral and decrease for the opposite spiral. (**B**) When Δt is compared to curvature, a steep increase in Δt is evident when curvature was about 0.16 cm^{-1}.

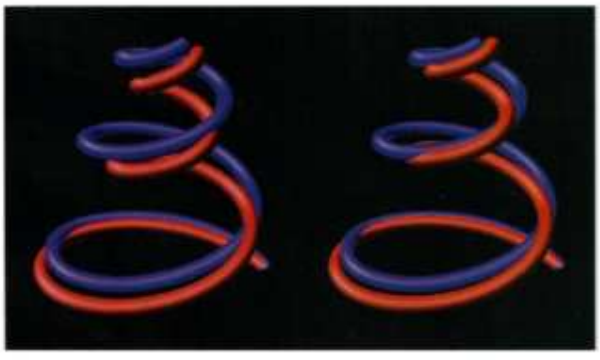

Fig. 3. Comparison of the finger trajectory and its cortical representation in time and space. The red path is formed from the population vectors, the blue from the movement vectors. Time is represented vertically and the other two dimensions are the horizontal and vertical directions of the drawing surface. The time axis of the spiral on the left is scaled in even increments. The time increments of the right spiral are adjusted by Δt. This results in a closer alignment of the red and blue paths, especially in the middle of the spiral where the curvature is highest. This spiral was drawn from the outside->in.

These findings provide evidence that cerebral processing operates dynamically in a distributed manner as in other vertebrate and invertebrate motor systems (*11*).

The finding that neurons coarsely encode a given parameter also supports a distributed organization. Individual neurons cannot accurately encode individual parameters, and this condition has generated population theories in which many neurons participate simultaneously. The resolution of the population code is better than a comparable code composed of individual neurons with narrow, discrete tuning. Coarse coding also makes it possible for a cell to encode more than one parameter simultaneously. Thus, a given neuron can participate in multiple populations representing different parameters.

REFERENCES AND NOTES

1. A. P. Georgopoulos, J. F. Kalaska, R. Caminiti, J. T. Massey, *J. Neurosci.* **2**, 1527 (1982).
2. A. P. Georgopoulos, R. Caminiti, J. F. Kalaska, J. T. Massey, *Exp. Brain Res. Suppl.* **7**, 327 (1983).
3. A. P. Georgopoulos, J. T. Lurito, M. Petrides, A. B. Schwartz, J. T. Massey, *Science* **243**, 234 (1989).
4. A. B. Schwartz, *J. Neurophysiol.* **70**, 28 (1993).
5. F. Lacquaniti, C. Terzuolo, P. Viviani, *Acta Psychol.* **54**, 115 (1983). The exact value of the exponent may vary with overall speed [J. Wann, I. Nimmo-Smith, A. M. Wing, *J. Exp. Psychol. Hum. Percept. Perform.* **14**, 622 (1988)] or in development [P. Viviani and R. Schneider, *J. Exp. Psychol.* **17**, 198 (1991)] where a stable value of ⅓ is not reached until the age of 12. This law has been shown to be valid in a wide range of arm and drawing movements.
6. An experiment performed under isometric conditions in which subjects exerted force on a stationary handle to produce closed figures such as ellipses and lemniscates showed that this law was not the result of mechanical properties of the arm, because the law was valid when no displacement occurred [J. T. Massey, J. T. Lurito, G. Pellizer, A. P. Georgopoulos, *Exp. Brain Res.* **88**, 685 (1992)].
7. A. B. Schwartz, *J. Neurophysiol.* **68**, 528 (1992).
8. These cells form a subset of those used in the description of a different drawing task, and the anatomical location of these cells is reported in (*7*). The task began when a 1.2-mm target circle appeared on the screen. The animal then placed its finger in the circle and held it there for a random period (200 to 600 ms). This circle was located either in the center or at the top of the screen and served as the starting point for a spiral that was drawn from the inside->out or from the outside->in. After the initial hold period, the spiral appeared on the screen and the circle jumped to a new position along the figure. The animal was required to drag its finger to the new location of the circle within 300 ms. Upon acquisition of the target, the target would immediately jump to the next of 40 positions along the figure. In this way the target always stayed ahead of the monkey's finger until the figure was completely drawn. This is not strictly a tracking task, because the animal had full view of the entire figure to be drawn and was free to trace the figure at its own pace provided that it acquired the moving target location within 300 ms. If the animal did not reach the target within this period or if it lifted its finger from the screen, the trial was aborted. After successful completion of the task, the animal was administered a liquid reward.
9. The occurrence times of each action potential were used to obtain a firing rate by breaking the tracing time into 100 bins starting at movement onset. This way of normalizing each trial was done so that corresponding bins from trials of different duration could be added. Population vectors were calculated

$$P_j = \sum_{i}^{348} w_{ij} C_i$$

for each bin j. $\boldsymbol{C}_i$ is the preferred direction of the i^{th} cell and w_{ij} is a weighting function given by

$$w_{ij} = \frac{d_{ij} - \overline{d}_i}{dmax_i - \overline{d}_i}$$

where d_{ij} is the square root–transformed discharge rate [see note 13 in (*3*)] for the i^{th} cell in the j^{th} bin, $dmax_i$ is the transformed maximum discharge rate for the cell, and $\overline{d}_i$ is the transformed geometric mean discharge rate of the cell. Breaking the data into 100 bins resulted in 100 population vectors and 99 velocity vectors. Comparisons between the population and movement vectors were made either by use of a spline function to extrapolate the velocity data to 100 bins or by use of only the first 99 population vectors.
10. The path curvature was calculated by a three-point method as the angle between successive vectors divided by the arc length between the first and last point. An average bin duration was calculated by taking the mean drawing time and dividing by the number of bins. Angular velocity in each bin was taken as the change in direction divided by the average bin duration. A polynomial equation with four coefficients ("Poly_Fit," PV-WAVE software from Visual Numerics Inc.) was used to fit the population and movement directions and magnitudes with a least-squared error.
11. A. Lundberg, *Exp. Brain Res.* **12**, 317 (1971); G. M. Edelman and V. B. Mountcastle, *The Mindful Brain* (MIT Press, Cambridge, MA, 1978); J. F. Kalaska and D. J. Crammond, *Science* **255**, 1517 (1992); K. V. Baev, V. B. Esipenko, Y. P. Shimansky, *Neuroscience* **43**, 237 (1991); G. Wittenberg and W. B. Kristan, *J. Neurophysiol.* **68**, 1693 (1992); S. R. Lockery and W. B. Kristan, *J. Neurosci.* **10**, 1811 (1990); M. W. Jung and B. L. McNaughton, *Hippocampus* **3**, 165 (1993).

12. I thank A. Kakavand for training the animals. A. Kakavand and J. L. Adams assisted in the experiments. Supported by the National Institutes of Health (grant NS-26375).

8 March 1994; accepted 25 May 1994

Endothelial NOS and the Blockade of LTP by NOS Inhibitors in Mice Lacking Neuronal NOS

Thomas J. O'Dell,* Paul L. Huang, Ted M. Dawson, Jay L. Dinerman, Solomon H. Snyder, Eric R. Kandel,† Mark C. Fishman

Long-term potentiation (LTP) is a persistent increase in synaptic strength implicated in certain forms of learning and memory. In the CA1 region of the hippocampus, LTP is thought to involve the release of one or more retrograde messengers from the postsynaptic cell that act on the presynaptic terminal to enhance transmitter release. One candidate retrograde messenger is the membrane-permeant gas nitric oxide (NO), which in the brain is released after activation of the neuronal-specific NO synthase isoform (nNOS). To assess the importance of NO in hippocampal synaptic plasticity, LTP was examined in mice where the gene encoding nNOS was disrupted by gene targeting. In nNOS$^-$ mice, LTP induced by weak intensity tetanic stimulation was normal except for a slight reduction in comparison to that in wild-type mice and was blocked by NOS inhibitors, just as it was in wild-type mice. Immunocytochemical studies indicate that in the nNOS$^-$ mice as in wild-type mice, the endothelial form of NOS (eNOS) is expressed in CA1 neurons. These findings suggest that eNOS, rather than nNOS, generates NO within the postsynaptic cell during LTP.

Although the induction of LTP in the CA1 region of the hippocampus occurs postsynaptically, presynaptic changes are thought to also contribute to the enhancement of synaptic strength (*1*). Thus, LTP at these synapses requires the release of a retrograde messenger that acts on the presynaptic terminals to increase transmitter release (*2*). A likely candidate retrograde messenger is NO (*3*), a membrane-permeant gas generated by the enzyme NOS (*4*). There are several isoforms of NOS that fall into two major classes: (i) inducible NOS present in macrophages and (ii) constitutive Ca^{2+}-regulated NOS, which includes two isoforms, endothelial (eNOS) and neuronal (nNOS) (*5*).

A number of observations are consistent with the possibility that NO is a retrograde messenger for LTP and that it is generated by a constitutive Ca^{2+}-regulated isoform, presumably the neuronal isoform (*3*). Acti-

T. J. O Dell and E. R. Kandel, Howard Hughes Medical Institute and Center for Neurobiology and Behavior, College of Physicians and Surgeons of Columbia University, New York, NY 10032, USA.
P. L. Huang and M. C. Fishman, Cardiovascular Research Center, Massachusetts General Hospital East and Harvard Medical School, Charlestown, MA 02129, USA.
T. M. Dawson, Department of Neurology and Department of Neuroscience, Johns Hopkins University Medical School, Baltimore, MD 21205, USA.
J. L. Dinerman and S. H. Snyder, Department of Neuroscience and Department of Medicine, Cardiology Division, Johns Hopkins University Medical School, Baltimore, MD 21205, USA.

*Present address: Department of Physiology, University of California at Los Angeles School of Medicine, Los Angeles, CA 90024, USA.
†To whom correspondence should be addressed.